Reconstruction of a function from its spherical (circular) means with the centers lying on the surface of certain polygons and polyhedra

Leonid Kunyansky

September 3, 2010

Abstract

We present explicit filtration/backprojection-type formulae for the inversion of the spherical (circular) mean transform with the centers lying on the boundary of some polyhedra (or polygons, in 2D). The formulae are derived using the double layer potentials for the wave equation, for the domains with certain symmetries. The formulae are valid for a rectangle and certain triangles in 2D, and for a cuboid, certain right prisms and a certain pyramid in 3D. All the present inversion formulae yield exact reconstruction within the domain surrounded by the acquisition surface even in the presence of exterior sources.

Introduction

The spherical mean Radon transform and related inversion formulae are important, in particular, for solving problems of thermo- and photo-acoustic tomography (TAT/PAT) [23, 24, 28]. In these modalities a region of interest (ROI) within a human body is subjected to a very short electromagnetic (EM) pulse which causes thermoelastic expansion of the tissues and generates an outgoing acoustic wave. The resulting acoustic pressure is measured by the detectors placed on a surface surrounding ROI. The initial pressure distribution $f(x)$ is not uniform: tumors absorb much more EM energy than healthy tissue and thus generate a much stronger signal. Hence, by recovering $f(x)$ one obtains valuable medical information.

Under certain simplifying assumptions the problem of finding the initial pressure can be re-stated as that of inverting the spherical mean Radon transform in 3D over spheres with centers lying at the measuring surface. A similar problem in 2D arises when instead of usual point-like detectors one measures the acoustic pressure with linear detectors [6, 31, 32]. A detailed discussion of the solvability, range conditions, and inversion techniques for the spherical mean transform in 2D and 3D can be found in [1–4, 11–13, 18–21, 33, 35–37] and references therein.

In the present paper we derive explicit inversion formulae for the spherical (or, in 2D, circular) mean transform for certain measurement surfaces with special symmetries. In general, such explicit formulae play an important role in inverse problems: they provide an important

theoretical insight and, in some cases, they serve as a starting point for the development of efficient reconstruction algorithms. For example, a very popular filtration/backprojection (FBP) algorithm (see, for example, [25]) is obtained as a result of discretization of one of the explicit inversion formulae for the 2D Radon transform.

For the spherical mean Radon transform the inversion formulae of the filtration/back-projection type are known only for special types of the acquisition surfaces. In particular, several different formulae for the spherical measuring surface have been found in [38, 40] (in 3D), in [11] (in odd dimensions), in [10] (in even dimensions), and in [21] (in arbitrary dimensions). A general family containing as particular cases all the above-mentioned formulae for a sphere, was derived in [26]. The so-called "universal" backprojection formula [40] (already mentioned above) holds not only for a spherical measuring surface, but also for a the surface of an infinite cylinder and for a plane [39, 40] (both in 3D). Other formulae for the planar acquisition are also known [6, 8, 9, 27, 29]. The existence of the FBP-type formulae for these three types of surfaces (and the absence of such formulae for other smooth surfaces) can be explained by certain symmetries common to a sphere, a plane, and a cylinder, as discussed in [20].

For other measuring surfaces there exist certain numerical techniques for solving the problems TAT/PAT (see [1, 20, 33, 35–37] and references therein); but the inversion formulae for such surfaces are not known. (The notable exception is the explicit general solution obtained in [1] for any closed surface; however, this solution is given in terms of functions of the wave operator rather than in a form of a closed form integro-differential expression). In the present paper we derive explicit FBP-type inversion formulae for the spherical mean transform with the centers lying on the surfaces of certain polyhedra (in 3D) or on the boundaries of certain polygons (for circular mean transform in 2D).

The paper is organized as follows. In Section 1 we provide a formal description of the problem and supply some introductory information. Next, in Section 2 we explicitly solve the time reversal problem for the wave equation in a cube or a square (in 2D) by means of the double layer wave potentials. Such a solution is possible due to certain symmetries of these regions. Next, in Section 3, from the explicit solution of the wave equation we derive FBP-type formulae for the inversion of the spherical (circular) mean transform with centers on the boundary of a cube (a square). The present inversion formulae have an interesting property of being insensitive to acoustic sources lying outside of the region surrounded by the acquisition surface, as discussed in Section 3.3. Numerical examples of image reconstructions obtained using our formulae are provided in Section 3.4. Finally, in Section 4 we apply the same methods to some other domains possessing the necessary symmetries. In 2D these include a rectangle and three types of triangles: an equilateral and a right isosceles triangles, and a triangle with the angles $\frac{\pi}{2}, \frac{\pi}{3}$ and $\frac{\pi}{6}$. In 3D our formulae extend to cuboids, right prisms whose base is one of the three triangles mentioned above, and a pyramid whose side faces are equal right isosceles triangles.

1 Formulation of the problem

Throughout the paper we assume that the source of the acoustic pressure is supported within a bounded region Ω, the detectors are placed on the boundary $\partial\Omega$, and the speed of sound is

constant and equal to 1 in the whole space $\mathbb{R}^n$. The time-dependent acoustic pressure $p(x,t)$ satisfies the wave equation

$$\begin{cases} p_{tt} = \Delta_x p, & t \geq 0, \quad x \in \mathbb{R}^n \\ p(x,0) = f(x), & p_t(x,0) = 0, \end{cases} \tag{1}$$

where initial pressure $f(x)$ is supported within Ω. The detectors measure the values $P(y,t)$ of the pressure on the boundary:

$$P(y,t) = p(y,t)|_{y \in \partial\Omega}, \quad t \in [0, \infty). \tag{2}$$

Our goal is to reconstruct $f(x)$ from measurements $P(y,t)$.

When the measurements are done using conventional point-like acoustic detectors, the above problem has to be solved in 3D setting. However, when the so-called line detectors are utilized [6, 31, 32], the 3D problem reduces to a set of similar 2D inverse problems for the wave equation, so from the practical point of view both 2D and 3D cases are of interest.

In the 3D case the measurements need only be done during the time interval $[0, \mathrm{diam}\Omega]$, since the signal vanishes after $t = \mathrm{diam}\Omega$ due to the Huygens principle [34]. In the 2D case, the values of $P(y,t)$ in the whole interval $t \in [0, \infty)$ are needed for the theoretically exact reconstruction, and we will assume that these values are known. (However, if $P(y,t)$ is known for all $t \in [0, \mathrm{diam}\Omega]$, the remaining values for the time interval $[\mathrm{diam}\Omega, \infty)$ can be explicitly reconstructed, see [30] and the discussion at the end of the next section).

1.1 Spherical means

The problem of finding $f(x)$ can also be re-formulated in terms of inverting the spherical mean transform. Indeed, in 3D the solution to the initial value problem (1) can be written in the form of the Kirchhoff formula

$$p(x,t) = \frac{\partial}{\partial t} t M(x,t), \tag{3}$$

where $M(x,r)$ are the spherical means of $f(x)$

$$M(x,r) = \frac{1}{4\pi} \int_{S^2} f(x + r\omega) d\omega,$$

and where S^2 is the unit sphere in 3D. Thus, using (2) one can relate the spherical means $M(y,t)$ to $P(y,t)$:

$$P(y,t) = \frac{\partial}{\partial t} t M(y,t),$$

and, taking into account that $M(y,0) = 0$, solve for $M(y,t)$

$$M(y,t) = \frac{1}{t} \int_0^t P(y,t') dt'.$$

Now the problem is reduced to finding function $f(x)$ from its spherical means $M(y,t)$ with centers on $\partial\Omega$.

3

Similarly, in 2D, one can introduce the circular means $m(x, r)$:

$$m(x, r) = \frac{1}{2\pi} \int_{S^1} f(x + r\omega) d\omega.$$

Now solution of (1) can be expressed through $m(x, r)$ by the formula

$$p(x, t) = \frac{\partial}{\partial t} \int_0^t \frac{m(x, r) r dr}{\sqrt{t^2 - r^2}},$$

and, in particular,

$$P(y, t) = \frac{\partial}{\partial t} \int_0^t \frac{m(y, r) r dr}{\sqrt{t^2 - r^2}}, \ y \in \partial\Omega. \tag{4}$$

The integral in the right hand side of the latter equation is the well known Abel transform whose inversion formula is also well known. Thus, circular means $m(y, r)$ can be found from $P(y, t)$ by the following formula

$$m(y, r) = \frac{2}{\pi} \int_0^r \frac{P(y, t) dt}{\sqrt{r^2 - t^2}},$$

which again leads to the problem of reconstructing $f(x)$ from its cylindrical means $m(y, r)$. (Since $m(y, r)$ vanish for $r > \text{diam}\Omega$, the knowledge of $P(y, t)$ in the time interval $t \in [0, \text{diam}\Omega]$ is sufficient to reconstruct $m(y, r)$ using the latter formula; moreover, values of $P(y, t)$ for $t > \text{diam}\Omega$ can now be recovered from $m(y, r)$ by equation (4).)

1.2   Reconstruction strategies

It is well known that the initial pressure $f(x)$ can be found by the time reversal, i.e. by solving the wave equation back in time. In particular, in the 3D case, since solution to (1) vanishes within Ω after $t = \text{diam}\Omega$ due to the Huygens principle, one can solve the following initial-boundary-value problem backwards in time :

$$\begin{cases} u_{tt} = \Delta_x u, & t \in [0, T], \quad x \in \Omega \subset \mathbb{R}^3, \\ u(x, T) = 0, & u_t(x, T) = 0, \\ u(y, t) = P(y, t), & y \in \partial\Omega, \\ T = \text{diam}\Omega. \end{cases} \tag{5}$$

Function $f(x)$ we seek to recover equals u at the moment 0:

$$f(x) = u(y, 0). \tag{6}$$

In 2D the solution to the wave equation does not vanish in a finite time, and therefore the initial condition should be replaced by the condition of the decrease at $t \to \infty$:

$$\begin{cases} u_{tt} = \Delta_x u, & t \in [0, \infty), \quad x \in \Omega \subset \mathbb{R}^2, \\ \lim_{T \to \infty} u(x, T) = 0, & \lim_{T \to \infty} u_t(x, T) = 0, \\ u(y, t) = P(y, t), & y \in \partial\Omega. \end{cases} \tag{7}$$

As in 3D, $f(x)$ is found using formula (6).

The above initial-boundary-value problems can be solved numerically using, for example, finite difference methods (e.g. [5, 7]). For certain acquisition surfaces methods based on eigenfunction expansion can also be very effective [22]. Our goal, however, is to obtain an explicit filtration/backprojection type formula for the solution. If the existing detectors could measure (in addition to the pressure) the normal derivative of the pressure, such an explicit analytic solution could have been represented, using the Green's formula, in the form of the double- and single- layer potentials. Unfortunately, the normal derivative is not known. Still, explicit representations of the solution of the wave equation by means of the double layer potential are possible for surfaces with certain symmetries, such as, for example, a sphere, a cylinder, and a plane. In fact, the so-called "universal backprojection formula" [40] for these surfaces can be interpreted as evaluation of a certain double layer potential.

In the next section we find explicit inversion formulae for the case when Ω is a cube (in 3D) or a square (in 2D). First, we obtain explicit solutions for the problems (5) and (7) in the form of the double layer potentials. These formulae allow us to reconstruct $f(x)$ from the measured values of the pressure $P(y, t)$; in Section 3 they also will be used to derive explicit filtration/backprojection time formulae for recovering $f(x)$ from its spherical (circular) means in these domains.

2 Explicit solution of the wave equation in a cube or a square

2.1 Double layer potentials

In 3D, the retarded free space Green's function $G^{3D+}(x, t)$ is given by the following formula [34]

$$G^{3D+}(x, t) = \frac{\delta(t - |x|)}{4\pi |x|};$$

it solves the equation

$$G_{tt}^{3D+} - \Delta_x G^{3D+} = \delta(t)\delta(|x|) \qquad (8)$$

subject to the radiation condition as $t \to \infty$. We will need the advanced Green's function $G^{3D-}(x, t)$,

$$G^{3D-}(x, t) = G^{3D+}(x, -t) = \frac{\delta(t + |x|)}{4\pi |x|}, \qquad (9)$$

that solves (8) back in time and satisfies the radiation condition as $t \to -\infty$.

The double- and single- layer potentials are frequently used in the theory of partial differential equations (see e.g. [34]). The wave potentials that solve the time dependent wave equation, were introduced in [14, 15] (see also [16]). We summarize below some of the basic properties of the wave potentials that will be needed for further use. (Here we sacrifice generality for simplicity and discuss only the properties that will be used later in the text).

Given a plane Π and a function $\varphi(y, t)$, $y \in \Pi$ which is continuous, twice differentiable in time and compactly supported in both variables, we introduce the (advanced) single layer

potential $U(x,t)$ and the double-layer potential $V(x,t)$ with the density $\varphi(y,t)$ as follows:

$$U(x,t) = \int_{\mathbb{R}^1} \int_{\Pi} \varphi(y,t')G^{3D-}(y-x,t-t')ds(y)dt', \tag{10}$$

$$V(x,t) = \int_{\mathbb{R}^1} \int_{\Pi} \varphi(y,t')\frac{\partial}{\partial n_y}G^{3D-}(y-x,t-t')ds(y)dt', \tag{11}$$

where n is the normal to Π, and $ds(y)$ is the standard area element. Note that both $U(x,t)$ and $V(x,t)$ satisfy the wave equation for all x outside Π; both potentials describe waves propagating (backwards in time) away from the support of φ, and they satisfy the radiation condition at infinity as $t \to -\infty$. Also, $V(x,t) = 0$ for all $x \in \Pi$, and due to the standard jump conditions [16]

$$\lim_{\varepsilon \to 0, \varepsilon > 0} V(y \pm \varepsilon n, t) = \pm\frac{1}{2}\varphi(y,t), \quad y \in \Pi.$$

Since $G^{3D-}(x,t)$ vanishes for positive values of t, equation (11) implies that if $\varphi(y,t)$ vanishes for $t > t_0$ then so does $V(x,t)$. Finally, since n is constant, using (9) $V(x,t)$ can be re-written as follows

$$V(x,t) = -\frac{1}{4\pi}n \cdot \nabla_x \int_{\Pi} \frac{\varphi(y,t+|y-x|)}{4\pi|y-x|}ds(y). \tag{12}$$

$$= -\frac{1}{4\pi}\operatorname{div}\int_{\Pi} n\frac{\varphi(y,t+|y-x|)}{4\pi|y-x|}ds(y).$$

We notice that, due to (12), (for a planar surface only),

$$V(x,t) = -n \cdot \nabla_x U(x,t). \tag{13}$$

In 2D, the advanced free space Green's function $G^{2D-}(x,t)$ has the following form [34]:

$$G^{2D-}(x,t) = \begin{cases} \frac{1}{2\pi\sqrt{t^2-x^2}}, & |x| < |t|, t < 0, \\ 0, & \text{otherwise} \end{cases}.$$

Further, for a given straight line L and for a continuous, twice differentiable in time, compactly supported in both variables function $\varphi(y,t)$, $y \in L$ we define the single-layer potential $U(x,t)$ with the density $\varphi(y,t)$:

$$U(x,t) = \int_L \int_t^{\infty} \varphi(y,t')G^{2D}(y-x,t-t')dt'dl(y)$$

$$= \frac{1}{2\pi}\int_L \int_{|x-y|}^{\infty} \varphi(y,t+\tau)\frac{1}{\sqrt{\tau^2-(x-y)^2}}d\tau dl(y)$$

$$= -\frac{1}{2\pi}\int_L \int_{|x-y|}^{\infty} \left(\frac{\partial}{\partial r}\frac{\varphi(y,r)}{r}\right)\Big|_{r=t+\tau} \sqrt{\tau^2-(x-y)^2}d\tau dl(y). \tag{14}$$

6

Now, instead of dealing directly with $\frac{\partial}{\partial n}G^{2D-}(x,t)$ (which would lead to strongly singular integrals), we define the double layer potential $V(x,t)$ by means of (13) and (14):

$$V(x,t) = -n \cdot \nabla_x U(x,t)$$

$$= \frac{1}{2\pi}n \cdot \nabla_x \int\limits_L \int\limits_{|x-y|}^{\infty} \left(\frac{\partial}{\partial r}\frac{\varphi(y,r)}{r}\right)\Bigg|_{r=t+\tau} \sqrt{\tau^2 - (x-y)^2}\,d\tau dl(y)$$

$$= -\frac{1}{2\pi} \int\limits_L \int\limits_{|x-y|}^{\infty} \left(\frac{\partial}{\partial r}\frac{\varphi(y,r)}{r}\right)\Bigg|_{r=t+\tau} n \cdot \nabla_y \sqrt{\tau^2 - (x-y)^2}\,d\tau dl(y)$$

$$= -\frac{1}{2\pi} \int\limits_L \int\limits_{|x-y|}^{\infty} \left(\frac{\partial}{\partial r}\frac{\varphi(y,r)}{r}\right)\Bigg|_{r=t+\tau} \frac{n \cdot (x-y)}{\sqrt{\tau^2 - (x-y)^2}}\,d\tau dl(y),$$

where n is the normal to L, and $dl(y)$ is the standard arc length. As before, $V(x,t)$ satisfies the wave equation (now in 2D) for all x outside L and it describes an outgoing wave propagating (backwards in time) away from the support of φ. Also, $V(x,t) = 0$ for all $x \in L$, and

$$\lim_{\varepsilon\to 0, \varepsilon>0} V(y \pm \varepsilon n, t) = \pm\frac{1}{2}\varphi(y,t), \quad y \in L.$$

2.2 Time reversal in a cube

An explicit solution to the initial-boundary-value problem (5) for the case when Ω is a cube can be obtained using the double layer potentials, as described below.

Without loss of generality let us assume that $\Omega = (-a,a) \times (-a,a) \times (-a,a)$, and boundary $\partial\Omega$ consists of six faces S_j, $j = 1, ..., 6$:

$$\partial\Omega = \bigcup_{j=1}^{6} S_j.$$

In this case the wave leaves Ω after time $T = \text{diam}\Omega = 2\sqrt{3}a$. Let us assume that $x = (x_1, x_2, x_3)$, and that the face S_1 lies in the plane $x_1 = a$. First. we will solve the initial-boundary-value problem with non-zero boundary conditions on face S_1 only:

$$\begin{cases} u_{tt} = \Delta_x u, \quad t \in [0,T], \quad x \in \Omega \subset \mathbb{R}^3, \\ u(x,T) = 0, \quad u_t(x,T) = 0, \\ \lim_{\varepsilon\to 0, \varepsilon>0} u(y - \varepsilon n_1, t) = P(y,t), \quad y \in S_1, \\ u(y,t) = 0, \quad y \in \bigcup_{j=2}^{6} S_j, \end{cases} \tag{15}$$

where n_1 is the exterior normal to S_1. The solution procedure we are about to outline will apply as well to the other faces S_j, $j = 2, ..., 6$, and the solution of problem (5) will then be readily obtained as the sum of the solutions corresponding to each face.

To simplify the presentation let us introduce an operator E^{2D} that extends any function $h(x_2, x_3)$ defined in the open square $(-a, a) \times (-a, a)$ to a function $h^{\mathrm{repl}}(x_2, x_3)$ defined in $\mathbb{R}^2$ by means of odd reflections. In detail, if $h^{\mathrm{repl}} = E^{2D}h$, then h^{repl} coincides with h within $(-a, a) \times (-a, a)$; further, for any point (x_2, x_3) lying in an open square $s_{n,m}$ with the side $2a$ and centered at $(2na, 2ma)$, $h^{\mathrm{repl}}(x_2, x_3)$ is defined by the following formula:

$$h^{\mathrm{repl}}(x_2, x_3) = (-1)^{m+n} h(a, (-1)^n (x_2 - 2na), (-1)^m (x_3 - 2ma)).$$

Finally, on the boundary of each square $s_{n,m}$ we define function $h^{\mathrm{repl}}(x_2, x_3)$ to be zero.

Let us denote by Π_1^a the plane containing S_1, and introduce plane Π_1^b parallel to Π_1^a and passing through the point $(-3a, 0, 0)$. We equip both planes with the same normal n_1 coinciding with the exterior normal to face S_1. We introduce function $P_1^{\mathrm{repl}}(x_2, x_3, t) = E^{2D}\left(P(x, t)|_{S_1}\right)$, i.e. we replicate the boundary values of u on face S_1. Now, for $t \in [0, T]$, we define the double-layer potentials $V_1^a(x, t)$ and $V_1^b(x, t)$ with the density $-2P_1^{\mathrm{repl}}(y_2, y_3, t)$ supported on planes Π_1^a and Π_1^b:

$$V_1^a(x, t) = \frac{1}{2\pi} \operatorname{div} \int\limits_{\mathbb{R}^2} \frac{n_1}{|(a, y_2, y_3) - x|} P_1^{\mathrm{repl}}(y_2, y_3, t + |(a, y_2, y_3) - x|) dy_2 dy_3,$$
$$V_1^b(x, t) = \frac{1}{2\pi} \operatorname{div} \int\limits_{\mathbb{R}^2} \frac{n_1}{|(-3a, y_2, y_3) - x|} P_1^{\mathrm{repl}}(y_2, y_3, t + |(-3a, y_2, y_3) - x|) dy_2 dy_3. \tag{16}$$

Note that since P_1^{repl} is finitely supported in $[0, T]$ in the time variable, the integrands in the above expressions vanish for large values of y_2 or y_3, and therefore the integration is actually performed over bounded subsets of $\mathbb{R}^2$ lying within the ball $B(x, T - t)$. In order to make expressions (16) simpler, we will abuse notation by writing $P_1^{\mathrm{repl}}(y, t)$ for $y \in \Pi_1^a$ or $y \in \Pi_1^b$ instead of $P_1^{\mathrm{repl}}(y_2, y_3, t)$:

$$V_1^{a,b}(x, t) = \frac{1}{2\pi} \operatorname{div} \int\limits_{\Pi_1^{a,b} \cap B(x, T-t)} \frac{n_1}{|y - x|} P_1^{\mathrm{repl}}(y, t + |y - x|) ds(y), \tag{17}$$

where $ds(y)$ is the standard area element, and $V_1^{a,b}$ means either V_1^a or V_1^b.

The combined potential $V_1(x, t) = V_1^a(x, t) + V_1^b(x, t)$ has some interesting properties. Let us denote by S_2 the face of cube Ω opposite to S_1. We notice that planes Π_1^a and Π_1^b are symmetric with respect to S_2, and, due to the choice of the normals, potential $V_1(x, t)$ vanishes on S_2. Next, due to the oddness of P_1^{repl}, potential $V_1(x, t)$ vanishes on the other four faces S_j of the cube $(j = 3, ..., 6)$. Finally, since T is smaller than the distance between Π_1^a and Π_1^b, potential $V_1^b(x, t)$ equals 0 on Π_1^a for all $t \leq T$. Therefore,

$$\lim_{\varepsilon \to 0, \varepsilon > 0} V_1(y - \varepsilon n_1, t) = \lim_{\varepsilon \to 0, \varepsilon > 0} V_1^a(y - \varepsilon n_1, t) = P(y, t), \quad y \in S_1.$$

Thus, potential $V_1(x, t)$ solves initial-boundary-value problem (15). For brevity, we will re-write the expression for $V_1(x, t)$ in the following form

$$V_1(x, t) = \frac{1}{2\pi} \operatorname{div} \int\limits_{(\Pi_1^a \cup \Pi_1^b) \cap B(x, T-t)} \frac{n_1}{|y - x|} P_1^{\mathrm{repl}}(y, t + |y - x|) ds(y).$$

In order to obtain the desired solution to (5), we replicate the boundary values on the faces $S_2, ..., S_6$:

$$P_j^{\text{repl}}(\cdot, \cdot, t) = E^{2D}\left(P(\cdot, t)|_{S_j}\right), j = 2, ..., 6. \tag{18}$$

Next, we introduce planes Π_j^a, Π_j^b with normals n_j, and define double layer potentials V_j with the densities $-2P_j^{\text{repl}}(y, t)$ on Π_j^a, Π_j^b:

$$V_j(x, t) = \frac{1}{2\pi} \operatorname{div} \int\limits_{(\Pi_j^a \cup \Pi_j^b) \cap B(x, T-t)} \frac{n_j}{|y-x|} P_j^{\text{repl}}(y, t + |y-x|) ds(y), \qquad j = 2, ..., 6.$$

The sum of these potentials $V(x, t) = \sum_{j=1}^6 V_j(x, t)$ solves the initial-boundary-value problem (5), and, therefore, $f(x)$ equals to $V(x, 0)$:

$$f(x) = \sum_{j=1}^6 V_j(x, 0) = \frac{1}{2\pi} \operatorname{div} \sum_{j=1}^6 \int\limits_{(\Pi_j^a \cup \Pi_j^b) \cap B(x, T)} n_j \frac{P_j^{\text{repl}}(y, |y-x|)}{|y-x|} ds(y). \tag{19}$$

Interestingly, while each of the potentials $V_j^{a,b}(x, t)$ solves the wave equation in the sense of distributions (due to the discontinuities in the edges of Ω) the sum $\sum_{j=1}^6 V_j(x, 0)$ of these potentials solves the wave equation in the classical sense (if $f(x) \in C_0^2(\Omega)$). Thus, we have proven the following

Theorem 1 *The $C_0^2(\Omega)$ initial condition $f(x)$ of the initial-boundary-value problem (1) in the case $n = 3$ can be reconstructed from the boundary values $P(y, t)$ (defined by (2)) by formulae (19) and (18).*

Formula (19) closely resembles the so-called "universal backprojection formula" [40] especially the version applicable to the measurements done over an infinite plane. However, in the present case the measurements are performed over a bounded surface (that of the cube), and the exact reconstruction at any point x is obtained by integration over a bounded set $B(x, T) \cap \bigcup_{j=1}^6 (\Pi_j^a \cup \Pi_j^b)$.

2.3 Time reversal in a square

A similar technique can be used to find the explicit solution to the initial-boundary-value problem (7) in the case when Ω is a square. The geometry of the problem is actually easier, thanks to the lower dimensionality of the problem. However, in 2D the Huygens principle does not hold and the solution will result from the integration over unbounded sets.

We will assume that Ω is a square $(-a, a) \times (-a, a)$, S_1 is the side of Ω corresponding to $x_1 = a$, and S_2 is the side contained by the line $x_1 = -a$.

First, let us find solution $u(x, t)$ to the following initial-boundary-value problem:

$$\begin{cases} u_{tt} = \Delta_x u, & t \in [0,T], \quad x \in \Omega \subset \mathbb{R}^2, \\ u(x,T) = 0, & u_t(x,T) = 0, \\ \lim_{\varepsilon \to 0, \varepsilon > 0} u(y - \varepsilon n, t) = P(y,t)\eta(T,t), & y \in S_1, \\ u(y,t) = 0, & y \in S_j, \quad j = 2,3,4, \end{cases} \tag{20}$$

where $\eta(T,t)$ is a C^∞ cut-off function equal 1 for $t \in [0, T-1]$ and vanishing with all the derivatives at $t = T$. We introduce operator E^{1D} that extends a function $h(x)$ defined in the interval $(-a, a)$, to a function $h^{\mathrm{repl}}(x)$ defined on $\mathbb{R}^1$ by means of odd reflections. In detail, within the interval $(-a, a)$ function h^{repl} coincides with h. For any $x \neq (2m+1)a$, $m \in \mathbb{Z}$, there is a unique integer $n(x)$ such that $|x - 2na| < a$. We define $h^{\mathrm{repl}}(x) = (-1)^{n(x)}h((-1)^{n(x)}(x - 2n(x)a))$. Finally, at the odd integer points h^{repl} vanishes: $h^{\mathrm{repl}}((2m+1)a) = 0$, $\forall m \in \mathbb{Z}$.

Let us call L_1 the straight line containing S_1. Introduce the family of lines Φ_1 consisting of all straight lines parallel to L_1, and passing through the points $(a + 4ka, 0)$, $k \in \mathbb{Z}$. (Obviously, $L_1 \in \Phi_1$). The exterior normal n_1 to the side S_1 of the square will be used as the normal to all the lines in Φ_1. Let us define function $P_1^{\mathrm{repl}}(x_2, t)$ by replicating values of $P(x,t)$ for $x \in S_1$:

$$P_1^{\mathrm{repl}}(x_2, t) = E^{1D}\left(P((a, x_2), t)\right).$$

We will abuse notation by writing $P_1^{\mathrm{repl}}(x,t)$ instead of the more accurate $P_1^{\mathrm{repl}}(x_2(x), t)$. Further, let us introduce the double layer potential $V_1(x,t,T)$ with the density $-2P_1^{\mathrm{repl}}(x_2, t)\eta(T,t)$ supported on all lines in the family Φ_1, defined by the formula

$$V_1(x,t,T) = \frac{1}{\pi} \int_{\Phi_1} \int_{|x-y|}^{\infty} \left(\frac{\partial}{\partial r} \frac{P_1^{\mathrm{repl}}(y,r)\eta(T,r)}{r} \right)\bigg|_{r=t+\tau} \frac{n_1 \cdot (x-y)}{\sqrt{\tau^2 - (x-y)^2}} d\tau \, dl(y).$$

Note that in the above formula the integration in y is actually performed over a bounded subset of Φ_1 due to the finite support of η in the second variable.

Potential $V_1(x,t,T)$ satisfies the wave equation in Ω. Since P_1^{repl} is odd with respect to the straight lines containing all sides of $\partial\Omega$, $V_1^T(x,t,T)$ vanishes on $\partial\Omega$. However, $V_1(x,t,T)$ is not continuous across S_1. The jump is such that

$$\lim_{\varepsilon \to 0, \varepsilon > 0} V_1(y - \varepsilon n_1, t, T) = P_1^{\mathrm{repl}}(y,t)\eta(T,t) = P(y,t)\eta(T,t), \quad y \in S_1, t \in [0.T].$$

Therefore, $V_1(x,t,T)$ solves the problem (20).

The next step is to obtain a solution $u^T(x,t)$ of the following boundary problem:

$$\begin{cases} u_{tt}^T = \Delta_x u^T, & t \in [0,T], \quad x \in \Omega \subset \mathbb{R}^2, \\ u^T(x,T) = 0, & u_t^T(x,T) = 0, \\ u^T(y,t) = P(y,t)\eta(T,t), & y \in \partial\Omega. \end{cases} \tag{21}$$

This can be achieved by defining functions $P_j^{\mathrm{repl}}(\cdot, t) = E^{1D}\left(P(\cdot, t)|_{S_j}\right)$ and families of parallel lines Φ_j with normals n_j, $j = 2, 3, 4$, and by introducing the corresponding double layer potentials $V_j(x,t,T)$, in a fashion similar to our definition of P_1^{repl}, Φ_1, n_1, and $V_1(x,t,T)$.

Now each $V_j(x, t, T)$ satisfies the boundary problem with the inhomogeneous conditions on the side j, and the homogeneous conditions on the other three sides of the square. In turn, the sum of these potentials u^T

$$u^T(x, t) = \sum_{j=1}^{4} V_j(x, t, T) = \frac{1}{\pi} \operatorname{div} \sum_{j=1}^{4} \left(\int_{0}^{T-t} \int_{\substack{\Phi_j \\ |y-x|<\tau}} n_j \frac{P_j^{\mathrm{repl}}(y, t+\tau)\eta(T, t+\tau)}{\sqrt{\tau^2 - (y-x)^2}} dl(y) d\tau \right)$$

$$= \frac{1}{\pi} \sum_{j=1}^{4} \int_{\Phi_j} \int_{|x-y|}^{\infty} \left(\frac{\partial}{\partial r} \frac{P_j^{\mathrm{repl}}(y, r)\eta(T, r)}{r} \right) \Bigg|_{r=t+\tau} \frac{n_j \cdot (x-y)}{\sqrt{\tau^2 - (x-y)^2}} d\tau dl(y)$$

solves (21).

It is known [17] that, as T grows to infinity, $u^T(x, 0)$ converges uniformly to $f(x)$:

$$f(x) = \lim_{T \to \infty} u^T(x, 0) = \lim_{T \to \infty} \frac{1}{\pi} \sum_{j=1}^{4} \int_{\Phi_j} \int_{|x-y|}^{\infty} \left(\frac{\partial}{\partial r} \frac{P_j^{\mathrm{repl}}(y, r)\eta(T, r)}{r} \right) \frac{n_j \cdot (x-y)}{\sqrt{r^2 - (x-y)^2}} dr dl(y)$$

$$\tag{22}$$

$$= \frac{1}{\pi} \sum_{j=1}^{4} \int_{\Phi_j} \int_{|x-y|}^{\infty} \left(\frac{\partial}{\partial r} \frac{P_j^{\mathrm{repl}}(y, r)}{r} \right) \frac{n_j \cdot (x-y)}{\sqrt{r^2 - (x-y)^2}} dr dl(y) \tag{23}$$

The latter formula is very similar to the explicit inversion formula for measurements done from an infinite line [6]. Formula (23) can also be re-written using the Green's function $G^{2D-}(x-y, r)$ to illustrate its connection to the surface potentials:

$$f(x) = \frac{1}{\pi} \sum_{j=1}^{4} \int_{\Phi_j} \int_{0}^{\infty} n_j \cdot (x-y) \left(\frac{\partial}{\partial r} \frac{P_j^{\mathrm{repl}}(y, r)}{r} \right) G^{2D-}(x-y, r) dr dl(y).$$

Theorem 2 *The $C_0^2(\Omega)$ initial condition $f(x)$ of the initial-boundary-value problem (1) in the case $n = 2$ can be reconstructed from the boundary values $P(y, t)$ (defined by (2)) by formulae (23).*

3 Explicit inversion of the spherical means: a cube and a square

3.1 Inversion formula in 3D

In 3D, in order to reconstruct $f(x)$ from its spherical means $M(y, t)$ with centers on $\partial\Omega$, we introduce replicated spherical means $M_j^{\mathrm{repl}}(y, t)$ defined as follows

$$M_j^{\mathrm{repl}}(\cdot, \cdot, t) = E^{2D} \left(M(\cdot, t)|_{S_j} \right), j = 1, ..., 6. \tag{24}$$

11

Since the replication operator E^{2D} is invariant with respect to the time variable, from (3) we conclude that

$$P_j^{\text{repl}}(y,t) = \frac{\partial}{\partial t} t M_j^{\text{repl}}(y,t). \tag{25}$$

Now formula for reconstructing $f(x)$ from spherical averages in 3D is obtained by substituting (25) into (19):

$$f(x) = \frac{1}{2\pi} \operatorname{div} \sum_{j=1}^{6} \int\limits_{(\Pi_j^a \cup \Pi_j^b) \cap B(x,T)} n_j \left(\frac{1}{t} \frac{\partial}{\partial t} t M_j^{\text{repl}}(y,t) \right)\Bigg|_{t=|x-y|} ds(y). \tag{26}$$

We thus have proven

Theorem 3 *In 3D, a $C_0^2(\Omega)$ function $f(x)$ supported within the cube Ω can be reconstructed from its spherical means $M(y,t)$ with centers on $\partial\Omega$ by the formula (26), where $M_j^{\text{repl}}(y,t)$ is defined by (24).*

Formula (26) has a form of the filtration by differentiation, followed by the backprojection, followed by the divergence operator. It is similar to the inversion formula obtained by the author [21] for the inversion of the spherical means with centers on a sphere (in 3D). In the latter case the integration is over the surface of a sphere, and no replication of the data is needed.

3.2 Inversion formula in 2D

In this section we derive an explicit inversion formula for finding $f(x)$ from the values of its circular means with the centers lying on the boundary of a square. The starting point for the derivation is equation (23) that reconstructs the sought function from the boundary values of the solution of the wave equation; we re-write it in the following form

$$f(x) = \frac{1}{\pi} \sum_{j=1}^{4} \int\limits_{\Phi_j} n_j \cdot (x-y) \left[\int\limits_s^\infty \left(\frac{\partial}{\partial r} \frac{P_j^{\text{repl}}(y,r)}{r} \right) \frac{1}{\sqrt{r^2 - s^2}} dr \right]\Bigg|_{s=|x-y|} dl(y)$$

$$= \frac{1}{\pi} \sum_{j=1}^{4} \int\limits_{\Phi_j} n_j \cdot (x-y) \hat{P}_j^{\text{repl}}(y,|x-y|) dl(y) \tag{27}$$

where

$$\hat{P}_j^{\text{repl}}(y,s) = \int\limits_s^\infty \left(\frac{\partial}{\partial r} \frac{P_j^{\text{repl}}(y,r)}{r} \right) \frac{1}{\sqrt{r^2 - s^2}} dr. \tag{28}$$

First, we will express $\hat{P}_j^{\text{repl}}(y,s)$ in terms of the circular averages $m(y,r)$. Let us apply the extension operator to $m(y,r)$ and define $m_j^{\text{repl}}(y,r)$ as follows:

$$m_j^{\text{repl}}(\cdot,r) = E^{1D}\left(m(\cdot,r)|_{S_j} \right), \qquad j = 1, ..., 4. \tag{29}$$

12

Function $P_j^{\text{repl}}(\cdot, t)$ is related to $m_j^{\text{repl}}(\cdot, r)$ in the same way as $P(\cdot, t)$ is related to $m(\cdot, r)$:

$$P_j^{\text{repl}}(y, t) = \frac{\partial}{\partial t} \int_0^t \frac{m_j^{\text{repl}}(y, r) r dr}{\sqrt{t^2 - r^2}} = \frac{\partial}{\partial t} \int_0^t \sqrt{t^2 - r^2} \frac{\partial}{\partial r} m_j^{\text{repl}}(y, r) dr = \int_0^t \frac{t \frac{\partial}{\partial r} m_j^{\text{repl}}(y, r)}{\sqrt{t^2 - r^2}} dr$$

$$= \int_0^t \frac{t \frac{\partial}{r \partial r} m_j^{\text{repl}}(y, r)}{\sqrt{t^2 - r^2}} r dr = \int_0^t \frac{\partial}{\partial r} \left(\frac{\partial}{r \partial r} m_j^{\text{repl}}(y, r) \right) t \sqrt{t^2 - r^2} dr,$$

where we integrated by parts twice, and used the fact that $m_j^{\text{repl}}(y, 0) = 0$ for all y. Now one can compute the derivative needed in (28):

$$\frac{\partial}{\partial t} \left(P_j^{\text{repl}}(y, t)/t \right) = \frac{\partial}{\partial t} \int_0^t \frac{\partial}{\partial r} \left(\frac{\partial}{r \partial r} m_j^{\text{repl}}(y, r) \right) \sqrt{t^2 - r^2} dr = t \int_0^t \frac{\frac{\partial}{\partial r} \left(\frac{\partial}{r \partial r} m_j^{\text{repl}}(y, r) \right)}{\sqrt{t^2 - r^2}} dr.$$

By substituting the above equation into (28), interchanging the integration order, and noticing that $m_j^{\text{repl}}(y, r) = 0$ for $r > 2\sqrt{2}a$, one obtains the following expression for $\hat{P}_{j,T}^{\text{repl}}(y, s)$:

$$\hat{P}_{j,T}^{\text{repl}}(y, s) = \lim_{T \to \infty} \int_s^T \int_0^t \frac{\partial}{\partial r} \left(\frac{\partial}{r \partial r} m_j^{\text{repl}}(y, r) \right) \frac{t}{\sqrt{t^2 - r^2} \sqrt{t^2 - s^2}} dr dt$$

$$= \lim_{T \to \infty} \int_0^{2\sqrt{2}a} \frac{\partial}{\partial r} \left(\frac{\partial}{r \partial r} m_j^{\text{repl}}(y, r) \right) \left[\int_{\max(s,r)}^T \frac{t}{\sqrt{t^2 - r^2} \sqrt{t^2 - s^2}} dt \right] dr$$

$$= \lim_{T \to \infty} \int_0^{2\sqrt{2}a} \frac{\partial}{\partial r} \left(\frac{\partial}{r \partial r} m_j^{\text{repl}}(y, r) \right) \left[\ln \left(\sqrt{T^2 - s^2} + \sqrt{T^2 - r^2} \right) - \frac{1}{2} \ln \left(|r^2 - s^2| \right) \right] dr$$

$$= -\frac{1}{2} \int_0^{2\sqrt{2}a} \ln \left(|r^2 - s^2| \right) \frac{\partial}{\partial r} \left(\frac{\partial}{r \partial r} m_j^{\text{repl}}(y, r) \right) dr$$

$$+ \lim_{T \to \infty} \int_0^{2\sqrt{2}a} \frac{\partial}{\partial r} \left(\frac{\partial}{r \partial r} m_j^{\text{repl}}(y, r) \right) \ln \left(\sqrt{T^2 - s^2} + \sqrt{T^2 - r^2} \right) dr \qquad (30)$$

The last integral in (30) vanishes:

$$\lim_{T \to \infty} \int_0^{2\sqrt{2}a} \frac{\partial}{\partial r} \left(\frac{\partial}{r \partial r} m_j^{\text{repl}}(y, r) \right) \ln \left(\sqrt{T^2 - s^2} + \sqrt{T^2 - r^2} \right) dr$$

$$= \lim_{T \to \infty} \int_0^{2\sqrt{2}a} \frac{\partial}{r \partial r} m_j^{\text{repl}}(y, r) \frac{r}{\left(\sqrt{T^2 - s^2} + \sqrt{T^2 - r^2} \right) \sqrt{T^2 - r^2}} dr = 0,$$

where we integrated by parts and used the finite support of $m_j^{\text{repl}}(y, r)$ in r. Now (30) can be re-written in the following form

$$\hat{P}_{j,T}^{\text{repl}}(y, s) = -\frac{1}{2} \int\limits_0^{2\sqrt{2}a} \ln\left(|r^2 - s^2|\right) \frac{\partial}{\partial r} \left(\frac{\partial}{r \partial r} m_j^{\text{repl}}(y, r)\right) dr = \text{PV} \int\limits_0^{2\sqrt{2}a} \frac{1}{r^2 - s^2} \frac{\partial}{\partial r} m_j^{\text{repl}}(y, r) dr,$$

where "PV" indicates that the integral is understood in the principal value sense. Substitution of the latter expression for $\hat{P}_{j,T}^{\text{repl}}(y, s)$ into (27) yields the following sequence of equivalent reconstruction formulae for $f(x)$:

$$f(x) = \frac{1}{\pi} \sum_{j=1}^4 \int\limits_{\Phi_j} n_j \cdot (x - y) \left(\text{PV} \int\limits_0^{2\sqrt{2}a} \frac{1}{r^2 - s^2} \frac{\partial}{\partial r} m_j^{\text{repl}}(y, r) dr\right)\Bigg|_{s=|x-y|} dl(y)$$

$$= -\frac{1}{2\pi} \sum_{j=1}^4 \int\limits_{\Phi_j} \frac{n_j \cdot (x - y)}{|x - y|} \left(\frac{\partial}{\partial s} \int\limits_0^{2\sqrt{2}a} \ln(|r^2 - s^2|) \frac{\partial}{\partial r} m_j^{\text{repl}}(y, r) dr\right)\Bigg|_{s=|x-y|} dl(y)$$

$$= \frac{1}{\pi} \sum_{j=1}^4 \int\limits_{\Phi_j} \frac{n_j \cdot (x - y)}{|x - y|} \left(\frac{\partial}{\partial s} \text{PV} \int\limits_0^{2\sqrt{2}a} \frac{r m_j^{\text{repl}}(y, r)}{r^2 - s^2} dr\right)\Bigg|_{s=|x-y|} dl(y) \qquad (31)$$

$$= \frac{1}{\pi} \sum_{j=1}^4 \int\limits_{\Phi_j} n_j \cdot \nabla_x \left(\text{PV} \int\limits_0^{2\sqrt{2}a} \frac{r m_j^{\text{repl}}(y, r)}{r^2 - s^2} dr\right)\Bigg|_{s=|x-y|} dl(y) \qquad (32)$$

$$= \frac{1}{\pi} \text{div} \sum_{j=1}^4 \int\limits_{\Phi_j} n_j \left[\text{PV} \int\limits_0^{2\sqrt{2}a} \frac{m_j^{\text{repl}}(y, r)}{r^2 - (x - y)^2} r dr\right] dl(y). \qquad (33)$$

Thus, the following statement holds:

Theorem 4 *In 2D, a $C_0^2(\Omega)$ function $f(x)$ supported within the square Ω can be reconstructed from its circular means $m(y, r)$ with centers on $\partial\Omega$ by the formula (33) (or, equivalently, by formulae (31) or (32)), where $m_j^{\text{repl}}(y, r)$ is defined by (29).*

Formula (33) closely resembles formula 8.19 [2] that reconstructs a function from its circular means centered on a circle.

The drawback of formulae (31)-(33) is that the integration has to be done over an unbounded set $\cup_{j=1}^4 \Phi_j$. However, by analyzing the expression in parentheses in (31) one can notice that the integrand of the outer integral decreases as $|x - y|^{-3}$ for large values of y. Moreover, for values of $|x - y| > 2\sqrt{2}a$ the integrand is infinitely smooth. Therefore, by integrating over a subset Φ^{trunc} containing all points $y \in \cup_{j=1}^4 \Phi_j$ such that $\text{dist}(y, \Omega) \leq \text{diam}\Omega$ one correctly reconstructs the singularities of $f(x)$, and obtains a good quantitative approximation to $f(x)$. This conclusion is supported by the numerical evidence presented in the next section.

3.3   Reconstruction in the presence of exterior sources

The time reversal reconstruction methods in TAT/PAT (i.e. methods based on the numerical solution of the wave equation backwards in time) have the following interesting property. If the support of the initial perturbation $f(x)$ has a part lying outside the region enclosed by the acquisition surface $\partial\Omega$, the time reversal still correctly reconstructs the part of $f(x)$ lying within Ω. In other words, the exterior sources do not affect the reconstruction within Ω [1, 22]. Since reconstruction methods based on the expansions in the series of the eigenfunctions of the Dirichlet Laplacian on Ω [1, 22] are theoretically equivalent to the time reversal, they also inherit the insensitivity to the exterior sources. On the other hand, all previously known filtration/backprojection-type inversion formulae for the spherical mean transform do not have this property: in the presence of an exterior source the reconstruction within Ω will be incorrect.

The present inversion formulae (and their generalizations in the following sections) are based on the explicit solution of the wave equation (by means of double layer potentials). Thus, they inherit from the time reversal methods the insensitivity to the exterior sources. A numerical example demonstrating accurate reconstruction in the presence of an exterior source is presented in the next section.

3.4   Numerical examples

An example illustrating reconstruction of a function from its spherical means with centers lying on the surface of a cube is presented in Figure 1. As a phantom we used a set of 25 characteristic functions of balls of various radii supported within the cube $(-1, 1) \times (-1, 1) \times (-1, 1)$. The centers of all the balls lied in the plane $x_3 = 0$. The cross section of our phantom by the latter plane is shown in Figure 1(a). The part (b) of this figure demonstrates the cross section of the image reconstructed on the grid of size $129 \times 129 \times 129$ using formula (26). The simulated detectors (i.e. the centers of the integration spheres) were placed on the uniform Cartesian 129×129 grids on each of the faces of the cube; there were 257 integration spheres for each detector with the radii varying uniformly from 0 to $2\sqrt{3}$. Our algorithm was based on a straightforward discretization of equation (26), where finite differences were used to compute the derivatives.

In order to illustrate the reconstruction in the presence of exterior sources we added to the phantom shown in Figure 1(a) a ball of radius 0.08 located at the position (1.1,0,0), and computed the spherical means corresponding to this extended set of sources. The size and location of this additional ball were chosen so that all the spherical means used for the reconstruction still vanished when the radii exceeded $2\sqrt{3}$. The result of the reconstruction computed using formula (26) is shown in Figure 1(c). The resulting image may seem indistinguishable from the one in Figure 1(b); in fact, the difference is about 4% in the L^∞ norm. (In the absence of the discretization error the images would exactly coincide).

In Figure 2 we demonstrate the reconstruction of a function in 2D from its circular means centered on the boundary of a square $(-1, 1) \times (-1, 1)$ using a modified formula (31), with the integration restricted to the subset Φ^{trunc} of $\cup_{j=1}^{4}\Phi_j$ contained within the disk of radius $3\sqrt{2}$ centered at the origin. (All the points y satisfying the condition $\text{dist}(y, \Omega) \leq \text{diam}\Omega$ are contained in Φ^{trunc}). The main goal of this experiment was to evaluate the effect of
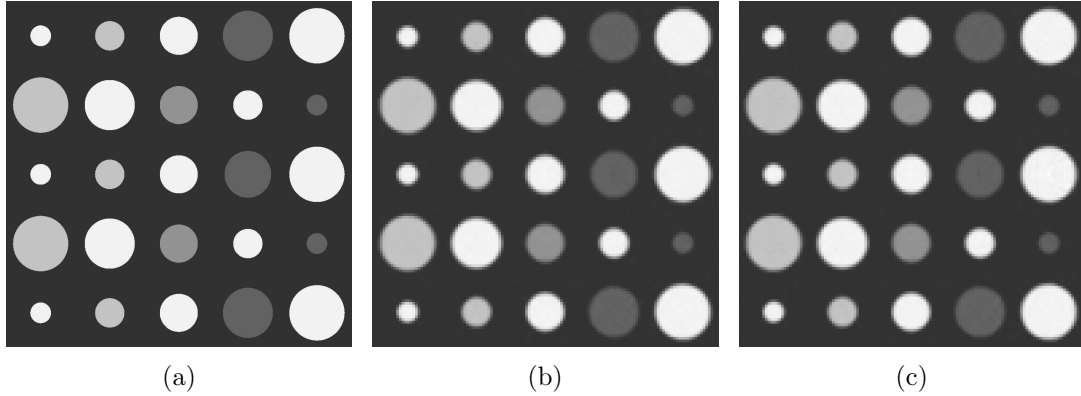
Figure 1: Reconstruction in 3D from spherical means centered on a surface of a cube (a) phantom (b) reconstructed function (c) reconstruction in a presence of a source outside of the cube
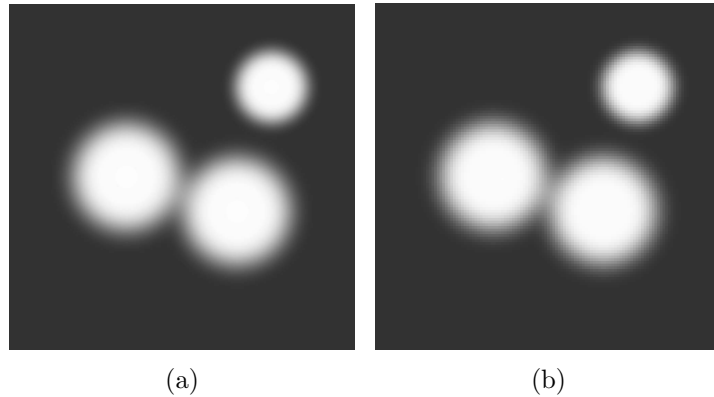

Figure 2: Reconstruction in 2D from circular means centered on the perimeter of a square (a) phantom (b) reconstruction

truncating the integration region. To this end we took care to eliminate other sources of error. In particular, as a phantom we chose a smooth function shown in Figure 2(a). Moreover, our implementation of formula (31) used a spectrally accurate algorithm for computing the Hilbert transform and a higher order polynomial interpolation during the backprojection. (The Hilbert transform arises since fraction $r/(r^2-s^2)$ in 31 can be re-written as $0.5/(r-s) + 0.5/(r+s)$.) The reconstructed function is shown in In Figure 2(b). The image is almost identical to the phantom; the relative reconstruction error in this example equals $7.4 \cdot 10^{-3}$ in the L^∞ norm. In other words, the truncation error is negligible for most practical applications, if all the points y satisfying the condition $\text{dist}(y, \Omega) \leq \text{diam}\Omega$ are included in the truncated domain.

16

4 Explicit inversion formulae for some other domains

4.1 Re-visiting the replication procedure for a cube and a square

The inversion formulae introduced in this paper for a cube (in 3D) and a square (in 2D) are based on the explicit representations of a solution of the wave equation by double-layer potentials. In general, double layer potentials are frequently used to solve Dirichlet problems for various PDE's in the interior and/or exterior of bounded regions. Usually such formulations lead to boundary integral equations for the potential densities that have to be solved numerically. However, as explained in the previous sections, if the detectors (centers of spherical means) are located on the boundary of a cube (or, in 2D, a square), the solution of the wave equation can be represented by the double layer potentials supported on certain periodic planes, with certain periodic densities. Due to the symmetries in these geometries, the potentials vanish on the planes, and the jump conditions relate the densities directly to the known boundary values, thus providing the desired explicit reconstruction formulae.

This approach can be extended to obtain explicit reconstruction formulae for the measurements made from the boundaries of certain polygons (in 2D) and polyhedra in (3D) possessing sufficient symmetries. These formulae will be similar to the present formulae for the square and the cube, but the planes supporting the potentials and the replication procedure defining the densities will be different in each case.

Before extending the inversion formulae to these new domains, let us provide an alternative description of the replication procedure for a square and a cube – such that it would be easier to generalize to other geometries. We start with a square, in 2D. Our goal is, again, to find the solution $u^T(x,t)$ of the initial-bouindary-value problem (21) provided the boundary values of u are known. To this end, let us construct a tesselation of the plane $\mathbb{R}^2$ by squares of the size $2a \times 2a$, one of which coincide with $\Omega = (-a,a) \times (-a,a)$. In each square we define u^{repl} to equal $\pm u^T$ (in some local coordinates). The signs are chosen so as to be different in any two adjacent squares. The local coordinates are defined in such a way that the function in any two adjacent squares is odd with respect to the joint side of these two squares. The resulting function $u^{\mathrm{repl}}(x,t)$ is continuous in x everywhere except the boundary of each square. At each point of the boundary it has a jump equal to a doubled negative limiting value of $u^{\mathrm{repl}}(x,t)$ as x approaches the boundary from the inside. Now we define the double layer potential supported on all lines containing the boundary of the squares, with the density equal to the jump in u^{repl}. This new procedure leads to the same double layer potentials as were described in Section 2.3, with the densities equal $-2P_j^{\mathrm{repl}}(x_2,t)\eta(T,t)$ on each family of lines Φ_j. The rest of the reconstructing procedure is the same.

Similarly, in order to obtain the double layer potential for a solution of the wave equation in a cube $\Omega = (-a,a) \times (-a,a) \times (-a,a)$, we tessellate the plane with shifted versions of Ω. In each shifted cube we define $u^{\mathrm{repl}}(x,t)$ as a reflected version of $u(x,t)$ with a sign opposite to the sign used in the neighboring cubes. The local coordinates in each cube are defined in such a way that $u^{\mathrm{repl}}(x,t)$ is odd with respect to each side of each cube. Now we define the double layer potentials supported on all planes that contain all faces of all cubes, with the density equal to the jump of $u^{\mathrm{repl}}(x,t)$ across the cube faces. This new procedure produces the same set of the double layer potentials as was utilized in the Section 2.2, and it leads to the same reconstruction formulae. Although the double layer potential described above is
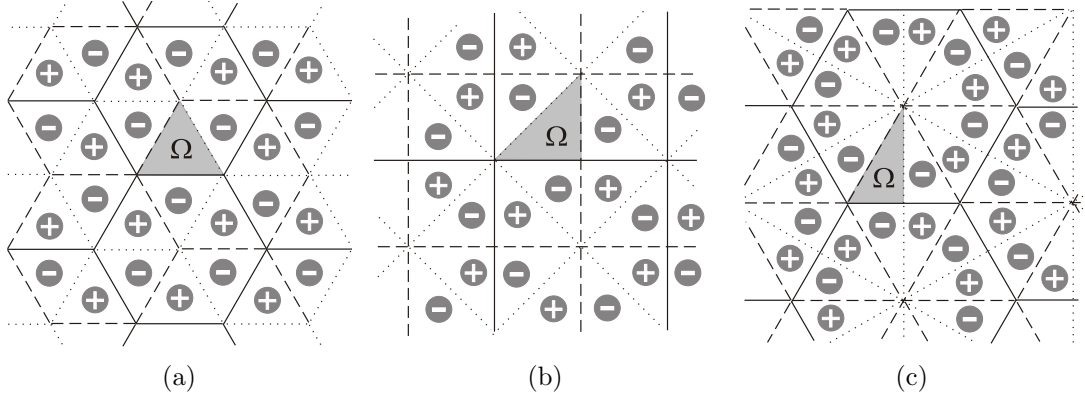
Figure 3: The tesselation schemes for some triangular domains (a) equilateral triangle (b) right isosceles triangle (c) triangle with angles $\frac{\pi}{2}, \frac{\pi}{3}$ and $\frac{\pi}{6}$

supported on an unbounded set, only a bounded subset of it is actually used to reconstruct the image within Ω, due to the finite speed of sound.

One obvious extension of the present inversion formulae is to rectangular domains in 2D and to cuboids in 3D. All the symmetries needed for the double layer potentials to form an explicit solution remain in place in these cases, and all the reconstruction formulae (for the wave equation and for the spherical/circular means) remain the same, with a proper re-definition of integration lines and planes.

4.2 Inversion formulae for certain triangular domains in 2D

In 2D, the inversion formulae presented in Sections 2.3 and 3.2 can be generalized to certain triangular domains. Namely, a equilateral triangle, a right isosceles triangle, and a triangle with the angles $\frac{\pi}{2}, \frac{\pi}{3}$ and $\frac{\pi}{6}$ can be used to tessellate the plane while preserving the necessary symmetries. The corresponding tesselations are shown in Figure 3. In each of the three cases shown in the figure, the sides of the triangular fundamental domain Ω are marked by different types of lines (solid, dashed, and dotted ones) so that the orientation of the local coordinates in each of the triangles is clear from the picture. Signs "+" and "-" indicate the choice of u or $-u$ in each triangle. Clearly, the resulting $u^{\text{repl}}(x, t)$ is odd with respect to all lines containing all sides of all the triangles. Therefore, if one defines the double layer potential with the density supported on these lines and equal to the jump of $u^{\text{repl}}(x, t)$ across the corresponding face, the value of this potential will vanish on all the triangle sides, and, due to the jump condition, this potential will solve the initial-boundary-value problem for the wave equation in Ω. Therefore, the analog of the formula (23) is valid with the corresponding re-definition of P^{repl} and with Ω being one of the above mentioned triangles.

This, in turn, allows us to obtain the analog of the inversion formulae (31) - (33) for the reconstruction from circular means, by defining m^{repl} in a similar fashion. As it is the case for the square domain, the latter formulae are exact if the integration is done over the unbounded graph. However, due to the fast decrease of the expression in the parentheses in (31) one can hope that the integration over the region containing all points y satisfying the condition $\text{dist}(y, \Omega) \leq \text{diam}\Omega$ will produce an accurate approximation to $f(x)$.
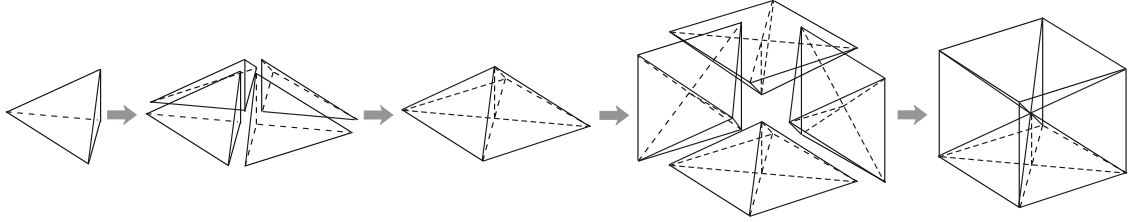
Figure 4: Extending $u(x, t)$ by odd reflections to a cube

4.3 Inversion formulae for certain polyhedral domains in 3D

In addition to cuboids, the techniques of the previous sections can also be used to find explicit solutions and inversion formulae in 3D for some other domains. In particular, one can derive explicit inversion formulae for reconstructing a function from its spherical means centered on the surface of a right prism of height H, whose base is one of the triangles discussed in the previous section. As before, it may be easier to start with finding the explicit solution to the wave equation $u(x, t)$ whose values on the boundary of the prism are known. In order to obtain such a solution, we replicate $u(x, t)$ in the directions parallel to the base of the prism, according to the schemes in Figure 3. Then we replicate the resulting slab of height H in the odd fashion with respect to the planes containing the bases of the prism, until $u(x, t)$ is extended to function $u^{\mathrm{repl}}(x, t)$ defined in the whole $\mathbb{R}^3$ in x. Further, we define the double layer potential with the density supported on planes containing the faces of all the replicated prisms, and equal to the jumps of $u(x, t)$ across the replicated faces. This double layer potential vanishes on all the faces, and, due to the jump condition, provides a solution to the initial-boundary-value problem for the wave equation in 3D. This results in an explicit formula analogous to (19). In order to obtain the analog of the formula (26) it is enough to define M^{repl} according to the replication procedure described above. Due to the Huygens principle, the integration is actually performed over the subset of the replicated faces satisfying the condition $|x - y| < \operatorname{diam}\Omega$; both formulae (for the spherical means and for the wave equation) are exact in this case.

Finally, the present method can be extended to the triangular pyramid Ω whose vertices have coordinates $(0, 0, 0), (a, 0, 0), (0, a, 0)$, and $(0, 0, a)$. (This region can also be described as a pyramid whose side faces are equal right isosceles triangles.) Again, starting with the solution $u(x, t)$ of the wave equation in Ω, we define $u^{\mathrm{repl}}(x, t)$ as follows. First, we reflect $u(x, t)$ in odd fashion with respect to the vertical faces of Ω to extend u to a rectangular pyramid (see Figure 4). Then we reflect (oddly) the pyramid with respect to its triangular faces to obtain six pyramids (only four are shown in the figure) to form a cube. Then the cube is used to tessellate the whole space. As before, we define the double layer potential by the jumps of the resulting function $u^{\mathrm{repl}}(x, t)$ across all the replicated faces. The symmetries of such an object guarantee that the potential vanishes on all the faces, and the jump conditions yield the required limiting values as one approaches the boundary of Ω from the inside. Thus, one obtains the exact solution to the initial-boundary-value problem corresponding to the time reversal of the wave equation. By implementing a similar replication procedure to define M^{repl}, one obtains an analog of the inversion formula (26) for reconstructing a function from

19

its spherical means centered on the surface of Ω.

It is worth noting that, similarly to the formulae for a cube and a square, all the formulae discussed in the present and previous sections also have the property of being insensitive to sources lying outside of the domain surrounded by the acquisition surface.

Conclusions

By utilizing the double layer wave potentials we found explicit solutions to the initial-boundary-value problems for the wave equation in certain 2D and 3D domains. In problems of TAT/PAT this yields explicit expressions for the result of the time reversal, and thus explicitly reconstructs the initial pressure distribution $f(x)$. Further, by formulating the problem in terms of spherical (circular) means, we obtain from the solutions to the wave equations explicit closed-form inversion formulae of filtration/backprojection type for the corresponding domains. In 2D, we presented inversion formulae for a square (or a rectangle), and we outlined their generalization for an equilateral triangle, right isosceles triangle, and a triangle with the angles $\frac{\pi}{2}, \frac{\pi}{3}$ and $\frac{\pi}{6}$. In 3D, we derived formulae for a cube (with immediate extension to a cuboid), and we discussed their generalization to right prisms whose bases are one of the three above-mentioned triangles, and to a pyramid whose side faces are equal right isosceles triangles.

In all cases the formulae for the inversion of the wave equation data are in the form of the double layer potentials supported on a series of planes, with the densities whose values equal to the known boundary values replicated according to the procedures described in the text. The formulae for inverting the spherical (or circular) means easily follow from the ones for the wave data. In the 3D case, due to the Huygens principle the integration in all the formulae is restricted to a bounded subset of the planes. In 2D, in order to obtain the exact reconstruction one has to integrate over an unbounded domain. However, our numerical experiments suggest that for a sufficiently accurate reconstruction it is enough to integrate over a bounded subset containing all points y satisfying the condition $\text{dist}(y, \Omega) \leq \text{diam}\Omega$.

Finally, all the presented inversion formulae remain exact within the domain even in the presence of sources located outside the domain. (In order to observe this phenomenon in 3D one may need to extend the measurement time (or the radii of the spherical means) to make sure that the signal vanishes after the observation time). Interestingly, although the time reversal and some series methods also have this property, the present formulae are the only known explicit FBP-type inversion formulae that exhibit such behavior.

References

[1] M. Agranovsky and P. Kuchment, Uniqueness of reconstruction and an inversion procedure for thermoacoustic and photoacoustic tomography with variable sound speed, *Inverse Problems* **23** (2007), 2089–2102.

[2] M. Agranovsky, P. Kuchment, and L. Kunyansky, On reconstruction formulas and algorithms for the thermoacoustic and photoacoustic tomography, Ch. 8 in [35], 89–101.

[3] M. Agranovsky, P. Kuchment, and E. T. Quinto, Range descriptions for the spherical mean Radon transform, *J. Funct. Anal.* **248** (2007), 344–386.

[4] M. Agranovsky and E. T. Quinto, Injectivity sets for the Radon transform over circles and complete systems of radial functions, *J. Funct. Anal.* **139** (1996), 383–414.

[5] G. Ambartsoumian and S. Patch. Thermoacoustic tomography: numerical results. Proceedings of SPIE 6437, *Photons Plus Ultrasound: Imaging and Sensing 2007: The Eighth Conference on Biomedical Thermoacoustics, Optoacoustics, and Acousto-optics*, Alexander A. Oraevsky, Lihong V. Wang, Editors, 64371B. 2007.

[6] P. Burgholzer, J. Bauer-Marschallinger, H. Grün, M. Haltmeier, and G. Paltauf, Temporal back-projection algorithms for photoacoustic tomography with integrating line detectors, *Inverse Problems* **23** (7) S65–S80.

[7] P. Burgholzer, G. J. Matt, M. Haltmeier, and G. Paltauf, Exact and approximative imaging methods for photoacoustic tomography using an arbitrary detection surface, *Phys Review E* **75** (2007) 046706.

[8] A. Denisjuk, Integral geometry on the family of semi-spheres, *J. Fractional Calculus and Appl. Anal.* **2**(2) (1999) 31–46.

[9] J. A. Fawcett, Inversion of n-dimensional spherical averages, *SIAM J. Appl. Math.* **45**(2) (1985) 336–341.

[10] D. Finch, M. Haltmeier, and Rakesh, Inversion of spherical means and the wave equation in even dimensions, *SIAM J. Appl. Math.* **68**(2) (2007) 392–412.

[11] D. Finch, S. Patch, and Rakesh, Determining a function from its mean values over a family of spheres, *SIAM J. Math. Anal.* **35** (2004), no. 5, 1213–1240.

[12] D. Finch and Rakesh, The spherical mean value operator with centers on a sphere, *Inverse Problems* **23** (2007), S37–S50.

[13] D. Finch and Rakesh, Recovering a function from its spherical mean values in two and three dimensions. In [35], 77–88.

[14] M. B. Friedman and R. Shaw, Diffraction of pulses by cylindrical obstacles of arbitrary cross section, *J. Appl. Mech. (Trans ASME)* **29** (1962) 40–46.

[15] W. Fulks and R. B. Guenther, Hyperbolic Potential Theory, Arch. Rational Mech. Anal., **49** (1972) 79–88.

[16] T. Ha-Duong, On Retarded Potential Boundary Integral Equations and their Discretization, in M. Ainsworth et al (Editors) *Topics in computational wave propagation: direct and inverse problems*, Lecture Notes in Computational Science and Engineering, **31**. Springer-Verlag, Berlin, (2003) 301–336.

[17] Y. Hristova, Time reversal in thermoacoustic tomography-an error estimate, *Inverse Problems,* **25** (2009) 055008.

[18] P. Kuchment, Generalized Transforms of Radon Type and Their Applications, in G. Olafsson and E. T. Quinto (Editors), *The Radon Transform, Inverse Problems, and Tomography,* Proc. Symp. Appl. Math. **63**, AMS, Providence, RI (2006) 67 – 91.

[19] P. Kuchment and L. Kunyansky, Mathematics of thermoacoustic tomography, *European J. Appl. Math.,* **19** (2008) Issue 02, 191–224.

[20] P. Kuchment and L. Kunyansky, Mathematics of Photoacoustic and Thermoacoustic Tomography, in *Handbook of Mathematical Methods in Imaging*, Springer, to appear.

[21] L. A. Kunyansky, Explicit inversion formulae for the spherical mean Radon transform, *Inverse Problems*, **23** (2007) 373–383.

[22] L. A. Kunyansky, A series solution and a fast algorithm for the inversion of the spherical mean Radon transform, *Inverse Problems*, **23** (2007) S11–S20.

[23] R. A. Kruger, P. Liu, Y. R. Fang, and C. R. Appledorn, Photoacoustic ultrasound (PAUS) reconstruction tomography, *Med. Phys.* **22,** (1995) 1605–1609.

[24] R. A. Kruger, D. R. Reinecke, and G. A.Kruger, GA Thermoacoustic computed tomography - technical considerations, *Med. Phys.* **26,** no. 9, (1999) 1832–1837.

[25] F. Natterer. *The mathematics of computerized tomography*, Wiley, New York, 1986.

[26] L. Nguyen, A family of inversion formulas in thermoacoustic tomography. *Inverse Problems and Imaging* **3**(4) (2009) 649–675.

[27] S. J. Norton, Reconstruction of a reflectivity field from line integrals over circular paths, *J. Acoust. Soc. Am.* **67**(3) 1980, 853–863.

[28] A. A. Oraevsky, S. L. Jacques, R. O. Esenaliev, and F. K. Tittel, Laser-based ptoacoustic imaging in biological tissues, *Proc. SPIE* 2134A (1994) 122–128.

[29] V. P. Palamodov, Reconstruction from limited data of arc means, *J. Fourier Anal. Appl.* **6**(1) (2000) 25–42.

[30] G. Paltauf, R. Nuster, M. Haltmeier, and P. Burgholzer. Photoacoustic Tomography With Integrating Area and Line Detectors. Ch. 20 in [35], 251–266.

[31] G. Paltauf, R. Nuster, M. Haltmeier, and P. Burgholzer. Thermoacoustic Computed Tomography using a Mach-Zehnder interferometer as acoustic line detector. *Appl. Opt.* **46**(16) (2007) 3352–8.

[32] G. Paltauf, R. Nuster, M. Haltmeier and P. Burgholzer. Experimental evaluation of reconstruction algorithms for limited view photoacoustic tomography with line detectors. *Inverse Problems* **23** (2007) S81–S94.

[33] S. K. Patch and O. Scherzer, Photo- and thermo-acoustic imaging (Guest Editors' Introduction), *Inverse Problems* **23** (2007) S01–S10.

[34] V. S. Vladimirov, *Equations of mathematical physics.* (Translated from the Russian by Audrey Littlewood. Edited by Alan Jeffrey.) Pure and Applied Mathematics, **3** Marcel Dekker, New York, 1971.

[35] L. H. Wang (Editor), *"Photoacoustic imaging and spectroscopy"*, CRC Press 2009.

[36] L. V. Wang and H. Wu, *"Biomedical Optics. Principles and Imaging"*, Wiley-Interscience 2007.

[37] M. Xu and L.-H. V. Wang, Photoacoustic imaging in biomedicine, *Review of Scientific Instruments* **77** (2006) 041101-01 – 041101-22.

[38] M. Xu and L.-H. V. Wang, Time-domain reconstruction for thermoacoustic tomography in a spherical geometry, *IEEE Trans. Med. Imag.* **21,** (2002) 814–822.

[39] M. Xu and L.-H. V. Wang, Time-Domain Reconstruction Algorithms and Numerical Simulations for Thermoacoustic Tomography in Various Geometries, *IEEE Trans. Biomed. Eng.* **50**(9) (2003) 1086–1099.

[40] M. Xu, L. V. Wang, Universal back-projection algorithm for photoacoustic computed tomography, *Phys Review E* **71** (2005) 016706.